Anal. Bioanal. Electrochem., Vol. 10, No. 5, 2018, 554-565

Analytical & Bioanalytical Electrochemistry

www.abechem.com

Full Paper

One-step Facile Preparation of High Performance $Ni(OH)_2$ Nanoparticles/Mesoporous Carbon Nanocomposite: Electrochemical Synthesis and Properties

Mustafa Aghazadeh*

Materials and Nuclear Research School, Nuclear Science and Technology Research Institute (NSTRI), P.O. Box 14395-836, Tehran, Iran

*Corresponding Author, Tel.: +982182064289

E-Mail: maghazadeh@aeoi.org.ir

Received: 14 March 2018 / Received in revised form: 28 April 2018 / Accepted: 30 April 2018 / Published online: 31 May 2018

Abstract- $Ni(OH)_2$ /mesoporous carbon composite was successfully deposited onto Ni foam by electrochemical deposition under ambient conditions. Using a simple electrochemical deposition (ECD) method, nickel hydroxide nanoparticles (NPs) was electrochemically formed onto mesoporous carbon structures (CMK). The surface morphology and crystallinity properties of the synthesized $Ni(OH)_2$ NPs/CMK onto Ni foam are characterized by physicochemical techniques of XRD and FE-SEM. Furthermore, the deposited β-$Ni(OH)_2$ NPs/CMK on Ni foam reveal superior energy storage ability in 1M KOH electrolyte as a binder-free electrode for pseudocapacitors. Compared to the $Ni(OH)_2$@NF electrode, the composite sample ($Ni(OH)_2$/CMK@ NF electrode) exhibit a relatively high electrochemical performance (*Cs*=1224 F g^{-1} at 2 A g^{-1}) and stable *Cs* retention (94%) after 3000 GCD cycling, which was ascribed to the electronic and ionic synergisms between β-$Ni(OH)_2$ NPs and mesoporous carbon material of Ni electrode. This cost-effective and *in situ* electrochemical growth of metal hydroxide nanostructures on carbonous structures may be useful for advanced energy storage device applications.

Keywords- $Ni(OH)_2$, Mesoporous carbon, Electrochemical synthesis, Nanoparticles, Electrochemical properties

1. INTRODUCTION

It is well-known that energy and power gaps between conventional physical capacitors and secondary batteries/fuel cells could be bridged by supercapacitors (SCs) [1]. Hence, supercapacitors have received extensive use in the fields of advanced electric vehicles and energy storage equipment. The high storage ability, long-cycle life and high-rate charge-discharging have made SCs as the powerful devises for use in many energy-related applications [2,3]. Nanostructured metal oxides [4-14] and hydroxides [15-21] have been reported to be proper electro-active compounds for SCs. These nanomaterials posses high specific capacitances (*Cs*) and long cycle life as compared with conventional carbonous materials due to their faradic charge-storage performances [23,24]. Among metal hydroxides, nickel hydroxide ($Ni(OH)_2$) with unique layered nano-structure has received increasing attention for use in supercapacitors [25-29]. Although, $Ni(OH)_2$ has been developed for pseudocapacitive applications, however, its practical application in SCs is still hindered by its poor conductivity. To address this problem, constructing hybrid materials with highly electrical conductive, flexible, and chemically stable conductive substrates have been reported to be promising approaches [30,31]. For example, compositing $Ni(OH)_2$ with carbon materials like as graphene [32,33], graphene oxide [34-36], CNTs [37,38], CMK [39,40], rGO [41,42], carbon fiber [43-45] and C_3N_4 [46-48] have been proposed and investigated. For example, Mi *et al.* reported reduced graphene oxide (RGO) on nickel hydroxide ($Ni(OH)_2$) film synthesized through hydrothermal approach [34]. They found that the RGO/$Ni(OH)_2$/Ni foam composite electrodes exhibited superior-capacitive ability with high capability (2500 $mFcm^{-2}$ at a current load of 5 mA cm^{-2}, or 1667 Fg^{-1} at 3.3 Ag^{-1}), compared with pure $Ni(OH)_2$/NF (450 mF cm^{-2} at 5 mA cm^{-2}, 409 Fg^{-1} at 3.3 Ag^{-1}) prepared under the identical conditions [34]. These results highlighted the importance of anchoring RGO films on nickel hydroxide surface for maximizing the electrochemical utilization of $Ni(OH)_2$ and graphene for energy storage application in supercapacitors. Hierarchically porous composite materials consisting of flake-like $Ni(OH)_2$ and mesoporous carbon have been synthesized by chemical precipitation method and exhibited excellent charge storage capability (*Cs*=2570 F/g) [40]. The improved electrochemical performance of $Ni(OH)_2$/mesoporous carbon composite has been attributed into the unique structure design in nickel hydroxide/mesoporous carbon composite in terms of its nanostructure, large specific surface area and good electrical conductance [40]. A facile and rapid electrophoretic deposition (EPD) approach has been also reported for the fabrication of reduced graphene oxide (RGO) and $Ni(OH)_2$ composite based on EPD of graphene oxide (GO) and $Ni(NO_3)_2$ colloidal suspension [42]. The resulting 100% binder-free RGO/$Ni(OH)_2$ electrodes have been exhibited excellent pseudocapacitive behavior with high specific capacitance of 1404 Fg^{-1} at 2 Ag^{-1}, high rate capability, and good electrochemical cycle life [42]. Furthermore, $Ni(OH)_2$ nanosheets have been grown on porous hybrid g-C_3N_4/RGO network and used as high

performance supercapacitor electrode [46]. This hybrid material have shown high supercapacitive performance (*Cs* of 1785 F/g at a current load of 2 A/g), desirable rate stability (retain 910 F/g at 20 A/g) and favorable cycling durability (*Cs* maintain of 71.3% after 5000 cycles at 3 A/g). Among the above mentioned carbonous materials, mesoporous carbon materials (CMK) have flexible structures and interconnected channels for the diffusion of electroactive species in electrochemical systems like as supercapacitors [48]. This unique feature of CMK can provide the proper electrolyte penetration, electrochemical usage of electro-active material, enhanced capacitances and charge/discharge rates for the CMK/metal hydroxide composites. Here, we developed one-step electrochemical synthesis procedure for facile fabrication of $Ni(OH)_2$/CMK nanocomposite. This procedure is based on the cathodic electro-deposition (CED) of nickel hydroxide from nickel nitrate aqueous solution with additive of CMK. It was reported that cathodic electro-synthesis provides a simple and short-time fabrication method for preparing the nanostructured metal hydroxides and oxides [49-55]. Hence, were applied this method in this research. In a typical two electrode deposition system containing 1 g/L CMK dispersed in 0.005 $Ni(NO_3)_2$ aqueous electrolyte, with applying DC mode (i=10 mA/cm^2) the expected composite ($Ni(OH)_2$/CMK) was deposited onto Ni foam. To the best of our knowledge, there is no report on the electrochemical preparation of $Ni(OH)_2$/CMK by this route. The prepared nanocomposite was characterized by various techniques of XRD, IR, FE-SEM and TGA. The results of these analyses confirmed the successful fabrication of CMK/$Ni(OH)_2$ composite. The electrochemical data obtained from cyclic voltammetry (CV) and galvanostatic charge-discharge (GCD) tests confirmed the excellent electrochemical performance of the prepared composite.

2. EXPERIMENTAL SECTION

2.1. Chemicals

$Ni(NO_3)_2.6H_2O$ (Merck) and KOH (Merck) were used as received. All solutions were prepared by using purified water prepared by a UHQ Elga System. An aqueous solution of 0.005 M $Ni(NO_3)_2.6H_2O$ was prepared and used as deposition bath.

2.2. Preparation of mesoporous carbon

Mesoporous carbon (CMK) was prepared according to the procedure reported in Ref. [56]. Briefly, sucrose (1.5 g), 0.5 cc sulfuric acid (Merck, 98%), 5cc water and 1g mesoporous silica were dissolved and the mixture was heated in oven for 5 h at 150 ^oC. Next, the obtained sample was pyrolyzed in N_2 atmosphere at 950 ^oC for 5 h to carbonize the polymer. In the last step, the silica template was removed by the dissolving in 5 wt% HF, where the pure mesoporous carbon (CMK) was achieved.

2.3. Electrochemical synthesis of $Ni(OH)_2$/CMK/NF composite

The electrodeposition solution was prepared through dissolving 1.15 g nickel nitrate ($Ni(NO_3)_2.6H_2O$) and 0.1 g CMK in 1 litter H_2O electrolyte. The electrochemical set up was composed of Ni foam (NF, 1 cm^2) cathode and graphite anode. The applied current density was 20 $mAcm^{-2}$. The deposition time and bath temperature were selected to be 10 min and 25 ^oC, respectively. After electrochemical synthesis, Ni foam electrode removed from the electrolyte and washed several times with the deionized water. Then this electrode was dried in oven at 70 ^oC for 2 h. Notably, it was measured that the electroactive material load on Ni foam was about 2.5 mg. The prepared electrode i.e. $Ni(OH)_2$/CMK/NF composite was characterized directly by FE-SEM and XRD techniques. Furthermore, it was directly used as binder-free working electrode in the electrochemical tests.

2.4. Characterization instruments

The surface morphology of the prepared Ni electrode was observed by field-emission scanning electron microscopy (FE-SEM, TE-SCAN model MIRA3 with accelerating voltage of 100 kV. The crystal structure of the working electrode was determined by XRD model Phillips PW-1800.

2.5. Electrochemical measurement

All the electrochemical measurements were performed by three-electrode system composed of Ag/AgCl reference electrode, $Ni(OH)_2$/CMK/NF composite (as working electrode) and counter electrode of platinum wire. These measurements included cyclic voltammetry (CV) and galvanostatic charge–discharge (GCD) tests, which were conducted on a potentiostat (AUTOLAB®, Eco Chemie, PGSTAT 30). An aqueous solution (i.e. 1 M KOH) was used as electrolyte in the above mentioned electrochemical tests. The CVs of the fabricated Ni working electrode were done at the potential range of -0.1 and 0.7 V *vs*. Ag/AgCl with applying the sweep rates of 2, 5, 10, 25, 50 and 100 mV s^{-1}. The capacitances (F/g) of the prepared $Ni(OH)_2$/CMK/NF composite were calculated using following formula [57]:

$$C = \int_{V_1}^{V_2} \frac{I}{m.\vartheta.\Delta V}\ dV \qquad (1)$$

Where I is the response current (A), *v* is the scan rate (V/s), *m* is the mass of electroactive materials in the electrodes (g), V is the potential (V). The GCDs were recorded at the currents of 1, 2, 3, 5 and 10 Ag^{-1} within a potential range of -0.1 to 0.45 V *vs*. Ag/AgCl. The calculations of Cs were conducted on the following formula [58]:

$$C = \frac{I \times \Delta t}{m \times \Delta V} \quad (2)$$

Where C is the specific capacitance for the prepared $Ni(OH)_2$/CMK/NF composite, I is the applied current load (A), ΔV is the potential range (V), Δt is the discharge time (s) and *m* is the mass of $Ni(OH)_2$/CMK onto Ni foam (g).

3. RESULTS AND DISCUSSION

3.1. Composite characterization

Fig. 1 presents the XRD patterns of the prepared CMK and its $Ni(OH)_2$/CMK/NF composite. As seen in Fig. 1a, two broad diffraction peaks for the prepared CMK at about 2θ of 23.5° and 43.5° are observed, corresponding to the (002) and (101) diffractions of graphite, which can be attributed to the semi-graphitized characterization of CMK-3 [59]. For the deposited CMK/nickel hydroxide onto Ni foam, two types of diffraction peaks are observable; i.e. three sharp peaks located at 2θ of 44.5°, 52.4° and 77.1° are attributed to Ni foam [60]. Furthermore, the peaks located at diffraction angels of 22.3°, 33.8°, 37.96° and 47.8°, corresponding to the facets of (100), (102), (110) and (111), respectively, which corresponds to the standard structure of $Ni(OH)_2$ (JCPDS #14-0117) [40].

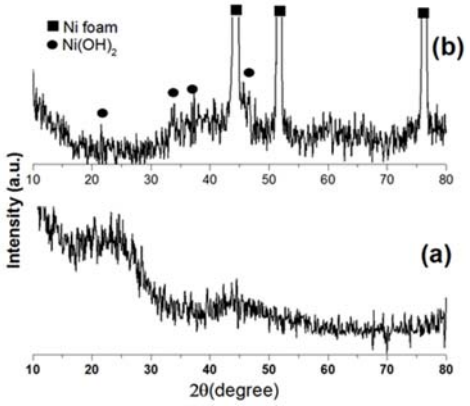

Fig. 1. XRD patterns of (a) CMK and (b) $Ni(OH)_2$/CMK@Ni foam

Fig. 2 displays the FE-SEM images of the prepared CMK and the electrodeposited $Ni(OH)_2$/CMK onto Ni foam. The prepared CMK was composed of micrometer-sized rod-like particles (Fig. 2a), and the rod-like morphology remained the highly ordered hexagonal arrangement of cylindrical mesoporous channels (Fig. 2b). Typical three dimensional Ni foam is also seen in Fig. 2c. For the prepared composite, it is seen that a thin film of deposit has been covered all the 3D interconnected channels of Ni foam (Fig. 2d), revealing the uniform condition in the electrodeposition of $Ni(OH)_2$/CMK/NF composite. The hydroxide part of

composite is uniformly grown onto CMK (Fig. 2e) and a layer of CMK is also covered the nickel hydroxides (Fig. 2f). Furthermore, it is seen that the nickel hydroxide deposit has particle morphology, which has spherical shape with mean sizes of 30 nm in diameter (Fig. 2g). The elemental analysis of the electrosynthesized composite onto Ni foam is provided in Fig. 2h.

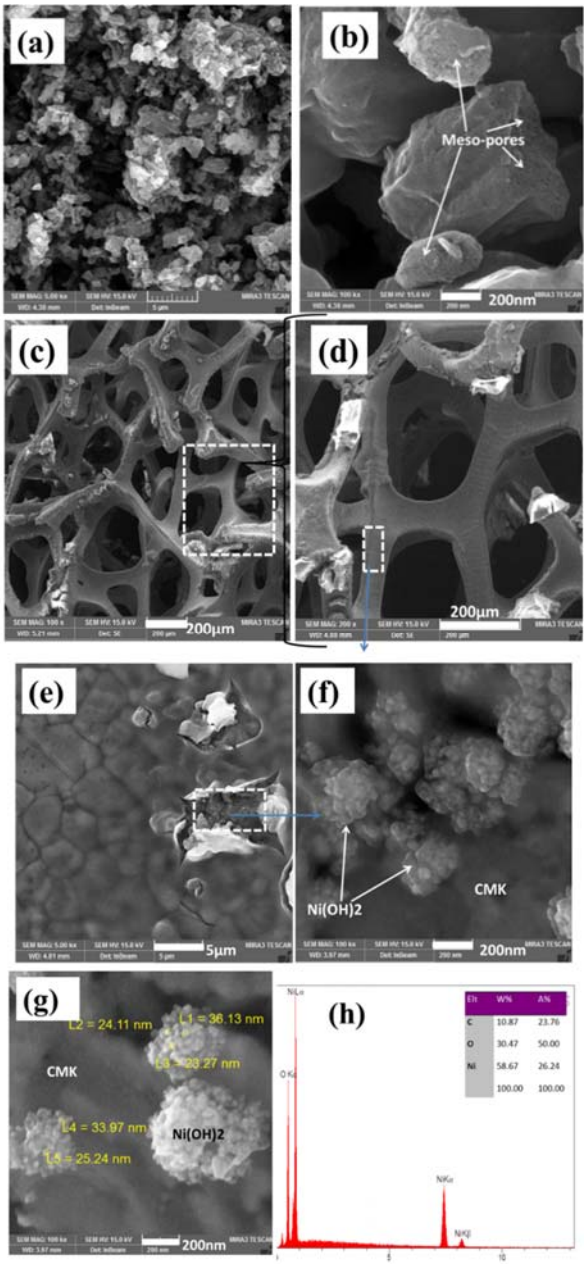

Fig. 2. FE- SEM images of (a,b) pristine CMK, (c-g) $Ni(OH)_2$/CMK@Ni foam and (h) its EDS data

It was found that the prepared composite has been composed of C, Ni and O elements with weight percentages of 23.7%, 26.24% and 50%, respectively. The $Ni(OH)_2$ part of composite was resulted from the presence of Ni and O elements, where the C element revealed the CMK part of the prepared $Ni(OH)_2$/CMK/NF composite.

3.2. Electrochemical evaluation

3.2.1. Cyclic voltammetry

Cyclic voltammograms of blank Ni foam, the deposited $Ni(OH)_2$ and $Ni(OH)_2$/CMK onto Ni foam in 1 M KOH electrolyte at the scan rate of 10 mV/s are presented in Fig. 3a. It is seen that the composite electrode ($Ni(OH)_2$/CMK/NF electrode) provides sharp redox peak and high current response as compare with both blank and $Ni(OH)_2$ deposited electrodes. This data revealed the role of CMK on the electrochemical performance of $Ni(OH)_2$, where it can be provided electric conductive substrate for the faradic reaction of $Ni(OH)_2$ part of working electrode [61-64]. Furthermore, the porous structure of CMK could facilitated the ionic movement and electrolyte penetration into the bulk part of $Ni(OH)_2$ [62,63].

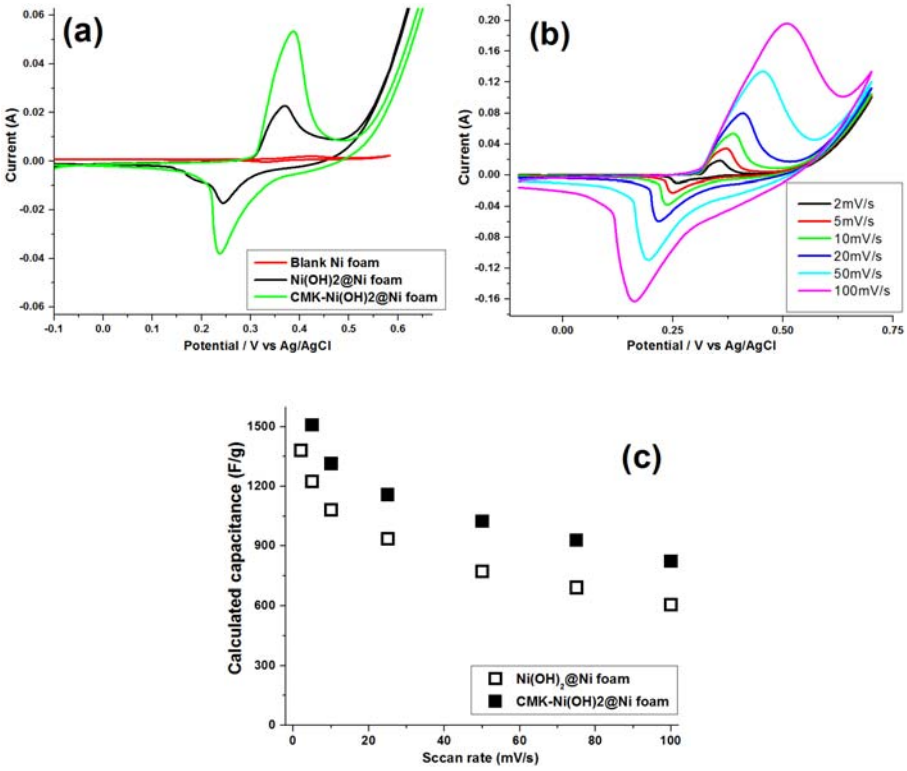

Fig. 3. (a) CVs of blank Ni foam, $Ni(OH)_2$@Ni and $Ni(OH)_2$/CMK@Ni electrodes at 10 mV/s, and **(b)** CVs of $Ni(OH)_2$/CMK@Ni foam at the various scan rates; **(c)** Its calculated capacitances *vs*. scan rate

Fig. 3b presents the CV profiles of the $Ni(OH)_2$/CMK/NF composite in 1 M KOH at the applied scan rates of 2, 5, 10, 25, 50, 75 and 100 mV s^{-1}. The CV contained one pair of Faradaic redox peaks. This form of CV curves showed that the capacitive performance of the nickel hydroxide composite electrode is mainly due to the pseudo-capacitance performance [63]. The observed redox peaks are corresponded to the following reactions [64]:

$$Ni(OH)_2 + OH^- \rightleftharpoons NiOOH + e^- \quad (3)$$

By Eq. (1), the Cs data of both electrodes were obtained and plotted versus scan rate as shown in Fig. 3c. The calculation revealed that our prepared $Ni(OH)_2$/CMK/NF composite is capable to exhibit the Cs value of 1780, 1590, 1315, 1159, 1025, 929 and 824 Fg^{-1} at the scan rates of 2, 5, 10, 25, 50, 75 and 100 mV s^{-1}, respectively. Notably, the electrosynthesized pure $Ni(OH)_2$@Ni electrode is capable to deliver Cs values of 1375, 1223, 1080, 937, 774, 691 and 606 Fg^{-1} at the scan rates of 2, 5, 10, 25, 50, 75 and 100 mVs^{-1}, respectively. Comparing the Cs values of these two electrodes showed that the supercapacitive performance of nickel hydroxide is greatly improved by composition with CMK.

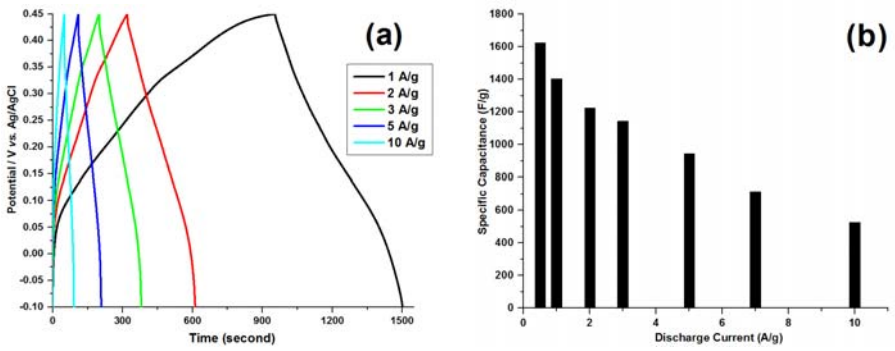

Fig. 4. (a) GCDs and **(b)** the calculated capacitances of the fabricated $Ni(OH)_2$/CMK/NF composite at different current loads

3.2.2. Charge-discharge tests

The $Ni(OH)_2$/CMK/NF composite was used as a binder-free electrode in a three-electrode system with 1 M KOH as electrolyte. The galvanostatic charge-discharge profiles of $Ni(OH)_2$/CMK@Ni electrode were measured at the current loads of 1, 2, 3, 5 and 10 Ag^{-1} and presented in Fig. 4a. All the curves have one plateau, revealing the pseudo-capacitive performance of the fabricated electrode. This plateau is ascribed to the redox reactions presented in Eq. (3). The Cs values of the fabricated $Ni(OH)_2$/CMK/NF composite were calculated using Eq. (2) and the results are plotted in Fig. 4b. The calculations give that our electrode has specific capacitances as high as 1385 Fg^{-1} (1 Ag^{-1}), 1224 Fg^{-1} (2 Ag^{-1}), 1143

Fg^{-1} (3 Ag^{-1}), 932 Fg^{-1} (5 Ag^{-1}) and 527 Fg^{-1} (10 Ag^{-1}). These values confirmed an excellent super-capacitive behavior for the electrosynthesized nanocomposite.

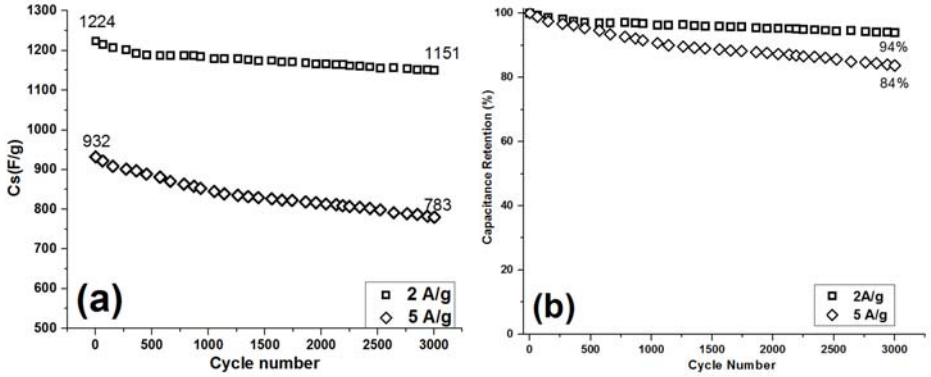

Fig. 5. Cycling performance of the synthesized $Ni(OH)_2$/CMK/NF composite at the current loads of 2 and 5 Ag^{-1}; (a) calculated Cs and (b) capacity retention *vs*. cycle number

To measure the cycling ability of $Ni(OH)_2$/CMK/NF composite in KOH electrolyte, this electrode was continuously cycled up to 3000 times at the current loads of 2 and 5 Ag^{-1}. The specific capacitances and their retentions at the applied loads were calculated and demonstrated in Fig. 5c. It was found that the *Cs* value of $Ni(OH)_2$/CMK/NF composite is reduced from 1224 Fg^{-1} to 1151 Fg^{-1}, which has cycle life of 94% after 3000 cycling at 2 Ag^{-1}. The delivered capacity at 5 Ag^{-1} was 783 Fg^{-1}, which has been reduced 16% as compared with its initial value i.e. 932 Fg^{-1}. This data indicated to retention of 84% capacity retention at high applied discharge rate.

4. CONCLUSION

The in situ and one-step electrochemical synthesis was developed for the fabrication of binder-free $Ni(OH)_2$/CMK/NF composite and its electrochemical performance as supercapacitor electrode was evaluated. The results of XRD and FE-SEM analyses proved that the electrosynthesized composite included beta nickel hydroxide nano-particles embedded into the mesoporous carbon structures. The elemental composition of the fabricated sample was studied by EDS data. The electrochemical performance (i.e. specific capacitance and cycle life) of the prepared composite was investigated using CV and GCD tests. The obtained electrochemical data confirmed the excellent charge storage of the $Ni(OH)_2$/CMK/NF composite.

Performed from the cobalt chloride containing starch, and the high surface area β-$Co(OH)_2$nano-sheets were obtained. The high surface area, β phase and sheet morphology of the electro-synthesized sample was specified through BET, XRD, IR, SEM and TEM

techniques. The CV and GCD test showed that the working electrode made from cobalt hydroxide nanosheets is capable to exhibit the high specific capacitances of 1120, 1024, 881, 735, 602 and 408 Fg^{-1} at the scan rates of 1, 2, 5, 10, 20, 50 and 100 mV s^{-1}, respectively. The values showed an excellent super-capacitive performance of the β-cobalt hydroxide nano-sheets, which resulted from their high surface area.

REFERENCES

[1] M. S. Whittingham, Proc. IEEE. 100 (2012) 1518.
[2] A. González, E. Goikolea, J. Andoni Barrena, and R. Mysyk, Renew. Sust. Energy Rev. 58 (2016) 1189.
[3] Q. Meng, K. Cai, Y. Chen, and L. Chen, Nano Energy 36 (2017) 268.
[4] M. Aghazadeh, M. G. Maragheh, M. R. Ganjali, and P. Norouzi, RSC Adv. 6 (2016) 10442.
[5] M. Aghazadeh, A. Bahrami-Samani, D. Gharailou, M. G. Maragheh, and M. R. Ganjali, J. Mater. Sci. 27 (2016) 11192.
[6] M. Aghazadeh, M. R. Ganjali, and P. Noruzi, Thin Solid Films 634 (2017) 24.
[7] M. Aghazadeh, and M.R. Ganjali, J. Mater. Sci.: Mater. Electron. 28 (2017) 8144.
[8] M. Aghazadeh, M. R. Ganjali, and P. Norouzi, J. Mater. Sci. 27 (2016) 7707.
[9] M. Aghazadeh, J. Mater. Sci. 28 (2016) 3108.
[10] M. Aghazadeh, and M. R. Ganjali, J. Mater. Sci. 53 (2018) 295.
[11] A. García-Gómez, S. Eugénio, R. G. Duarte, T. M. Silva, and M. F. Montemor, Appl. Surf. Sci. 382 (2016) 34.
[12] M. Aghazadeh, R. Ahmadi, D. Gharailou, M. R. Ganjali, and P. Norouzi, J. Mater. Sci. 27 (2016) 8623.
[13] A. Elmouwahidi, E. Bailón-García, and J. Castelo-Quibén, A. F. Pérez-Cadenas, F. J. Maldonado-Hódar, and F. Carrasco-Marín, J. Mater. Chem. A 6 (2018) 633.
[14] M. Aghazadeh, I. Karimzadeh, and M. R. Ganjali, J. Mater. Sci. 28 (2017) 13532.
[15] M. Aghazadeh, Mater. Lett. 211 (2018) 225.
[16] M. Aghazadeh, J. Mater. Sci. 28 (2017) 18755.
[17] S. Sepahvand, S. Ghasemi, and Z. Sanaee, Nano (2016) 1750010.
[18] M. Aghazadeh, A. A. M. Barmi, D. Gharailou, M. H. Peyrovi, and B. Sabour, Appl. Surf. Sci. 283 (2013) 871.
[19] M. Aghazadeh, and M. R. Ganjali, J. Mater. Sci. 28 (2017) 11406.
[20] J. Talat Mehrabad, M. Aghazadeh, M. Ghannadi Maragheh, and M. R. Ganjali, Mater. Lett. 184 (2016) 223.
[21] M. Aghazadeh, S. Dalvand, and M. Hosseinifard, Ceram. Int. 40 (2014) 3485.
[22] M. Aghazadeh, and S. Dalvand, J. Electrochem. Soc. 161 (2014) D18.
[23] C. Sasirekha, and S. Arumugam, AIP Conference Proceedings 1832 (2017) 050047.

[24] F. Shi, L. Li, X. Wang, C. Gu, and J. Tu, RSC Adv. 4 (2014) 41910.
[25] R. S. Kate, S. A. Khalate, and R. J. Deokate, J. Alloys Compd. 734 (2018) 89.
[26] M. Aghazadeh, B. Sabour, M. R. Ganjali, and S. Dalvand, Appl. Surf. Sci. 313 (2014) 581.
[27] M. Hwang, J. Kang, K. Seong, D. Kyom Kim, X. Jin, W. H. Antinka, C. Lee, and Y. Piao, Electrochim. Acta 270 (2018) 156.
[28] J. Tizfahm, B. Safibonab, M. Aghazadeh, A. Majdabadi, and B. Sabour, Colloids Surf. A 443 (2014) 544.
[29] T. Nguyen, M. Boudard, M. J. Carmezim, and M. F. Montemor, Scientific Reports 7 (2017) 39980.
[30] J. Li, M. Wei, W. Chu, and N. Wang, Chem. Eng. J. 316 (2017) 277.
[31] P. Sirisinudomkit, P. Iamprasertkun, A. Krittayavathananon, T. Pettong, P. Dittanet, and M. Sawangphruk, Scientific Reports 7, (2017) 1124
[32] N. Li, X. Huang, R. Li, Y. Chen, Y. Li, Z. Shi, and H. Zhang, Electrochim. Acta 219 (2016) 61.
[33] H. Yan, J. Bai, J. Wang, X. Zhang, B. Wang, Q. Liu, and L. Liu, CrystEngComm. 15 (2013) 10007.
[34] S. Min, C. Zhao, G. Chen, and X. Qian, Electrochim. Acta 115 (2014) 155.
[35] Z. Yang, C. Fang, Y. Fang, Y. Zhou, and F. Zhu, Int. J. Electrochem. Sci. 10 (2015) 1574.
[36] H. J. Loa, and H. Y. Chen, ECS Trans. 80 (2017) 453.
[37] R. R. Salunkhea, J. Lin, V. Malgras, S. X. Dou, J. H. Kim, Y. Yamauchi, Nano Energy 11 (2015) 211.
[38] H. Yi, H. Wang, Y. Jing, T. Peng, Y. Wang, J. Guo, Q. He, Z. Guo, and X. Wang, J. Mater. Chem. A 3 (2015) 19545.
[39] Y. Wang, D. Zhou, D. Zhao, M. Hou, C. Wang, and Y. Xia, J. Electrochem. Soc. 160 (2013) A98.
[40] J. Zhang, L.-B. Kong, J.J. Cai, H. Li, Y.C. Luo, and L. Kang, Micro. Meso. Mater. 132 (2010) 154.
[41] H. Ma, J. He, D. B. Xiong, J. Wu, Q. Li, V. Dravid, and Y. Zhao, ACS Appl. Mater. Interfaces 8 (2016) 1992.
[42] H. Zhang, X. Zhang, D. Zhang, X. Sun, H. Lin, C. Wang, and Y. Ma, J. Phys. Chem. B 117 (2013) 1616.
[43] L. Huang, D. Chen, Y. Ding, S. Feng, Z. L. Wang, and M. Liu, Nano Lett. 13 (2013) 3135.
[44] L. Huang, D. Chen, Y. Ding, Z. Lin Wang, Z. Zeng, and M. Liu, ACS Appl. Mater. Interfaces 5 (2013) 11159.

[45] L. Gao, J. U. Surjadi, K. Cao, H. Zhang, P. Li, S. Xu, C. Jiang, J. Song, D. Sun, and Y. Lu, ACS Appl. Mater. Interfaces 9 (2017) 5409.
[46] L. Li, J. Qin, H. Bi, S. Gai, F. He, P. Gao, Y. Dai, X. Zhang, D. Yang, and P. Yang, Scientific Reports 7 (2017) 43413.
[47] B. Dong, M. Li, S. Chen, D. Ding, W. Wei, G. Gao, and S. Ding, ACS Appl. Mater. Interfaces 9 (2017) 17890.
[48] A. Eftekhari, and Z. Fan, Mater. Chem. Front. 1 (2017) 1001.
[49] M. Aghazadeh, T. Yousefi, and M. Ghaemi, J. Rare Earths 30 (2012) 236.
[50] I. Karimzadeh, H. R. Dizaji, and M. Aghazadeh, J. Magn. Magn. Mater. 416 (2016) 81.
[51] M. Aghazadeh, A. A. M. Barmi, H. M. Shiri, and S. Sedaghat, Ceram. Int. 39 (2013) 1045.
[52] M. Aghazadeh, A. A. Malek Barmi, and M. Hosseinifard, Mater. Lett. 73 (2012) 28.
[53] M. Aghazadeh, M. G. Maragheh, M. R. Ganjali, and P. Norouzi, Inorg. Nano-Metal Chem. 27 (2017) 1085.
[54] M. Aghazadeh, I. Karimzadeh, and M. R. Ganjali, J. Electron. Mater. 47 (2018) 3026.
[55] M. Aghazadeh, and M. R. Ganjali, J. Mater. Sci. 29 (2018) 2291.
[56] L. Samiee, S. Tasharrofi, S. Sadegh Hassani, M. Fardi, and B. Mazinani, Curr. Nanosci. 13 (2017) 595.
[57] H. Liu, T. Yu, D. Su, Z. Tang, and Q. Kong, Ceram. Int. 43 (2017) 14395.
[58] R. Wang, P. Liu, J. Lang, L. Zhang, and X. Yan, Energy Storage Mater. 6 (2017) 53.
[59] C. Zheng, M. Liu, W. Chen, L. Zeng, and M. Wei, J. Mater. Chem. A 4 (2016) 13646.
[60] Y. Nie, H. Yang, J. Pan, W. Li, Y. Sun, and H. Niu, Electrochim. Acta 252 (2017) 558.
[61] J. Choi, M. Kim, and J. Kim, Ionics 24 (2018) 815.
[62] H. Jiang, J. Ma, and C. Li, Adv. Mater. 24 (2012) 4197.
[63] J. Feng, J. Zhao, B. Tang, P. Liu, and J. Xu, J. Solid State Chem. 183 (2010) 293.
[64] J. Ji, L. L. Zhang, H. Ji, Y. Li, X. Zhao, X. Bai, X. Fan, F. Zhang, and R. S. Ruoff, ACS Nano 7 (2013) 6237.